Structural Engineering and Mechanics, *Vol. 64, No. 6 (2017) 723-730*
DOI: https://doi.org/10.12989/sem.2017.64.6.723

Surface effects on flutter instability of nanorod under generalized follower force

Qiu-Xiang Xiao[1], Jiaqi Zou[1], Kang Yong Lee[2] and Xian-Fang Li[*1,2]

[1]*School of Civil Engineering, Central South University, Changsha 410075, PR China*
[2]*State Key Laboratory of Structural Analysis for Industrial Equipment and Department of Engineering Mechanics, Dalian University of Technology, Dalian 116024, PR China*

(Received May 3, 2017, Revised July 12, 2017, Accepted July 13, 2017)

Abstract. This paper studies on dynamic and stability behavior of a clamped-elastically restrained nanobeam under the action of a nonconservative force with an emphasis on the influence of surface properties on divergence and flutter instability. Using the Euler-Bernoulli beam theory incorporating surface effects, a governing equation for a clamped-elastically restrained nanobeam is derived according to Hamilton's principle. The characteristic equation is obtained explicitly and the force-frequency interaction curves are displayed to show the influence of the surface effects, spring stiffness of the elastic restraint end on critical loads including divergence and flutter loads. Divergence and flutter instability transition is analyzed. Euler buckling and stability of Beck's column are some special cases of the present at macroscale.

Keywords: surface elasticity; flutter instability; divergence instability; nanocantilever; elastically restrained end

1. Introduction

With the development of nanotechnology, nanomaterials and nanostructures have led to increasing applications of MEMS/NEMS (Zang *et al*. 2015). At micro/nanometer scale, material or structure exhibits mechanical behaviors different from those in macroscopic scale or in bulk. For 1D nanoscale structures, such as nanowires, nanorods and nanotubes, when the characteristic dimension of 1D nanoscale structures shrinks to microns or nanometers, the surface effects play a significant role in affecting their mechanical properties, and a possible reason is dramatic increasing of specific surface area (Cuenot *et al*. 2004, Jing *et al*. 2006, Moon and Hwang 2008). Therefore, much attention has been directed towards the investigation of surface effects in micro/nano materials and structures. In this field, Wang *et al*. gave a comment and summarized progress in a review paper (Wang *et al*. 2011), which contains many papers published before 2011.

In order to explain the effects of surface stress and surface elasticity on mechanical behaviors, in particular for vibration frequencies, considerable work has been reported in recent decades. For instance, a theoretical analysis of the influences of surface stress on the deflections and frequencies of rectangular AFM cantilever plates was given (Lachut and Sader 2007). Wang and Feng (2007) examined the effects of surface stresses as well as surface elasticity on the natural frequency of nanobeams. Park (2008) presented the coupled effects of surface stress and boundary conditions on the resonant properties of silicon nanowires. Shi *et al*. (2012) demonstrated the effects of surface stress on the bending stiffness of cantilever beams. Li *et al*. (2014) gave a theoretical analysis of the surface effect on apparent Young's modulus or bending stiffness adopting the Timoshenko beam theory with consideration of shear deformation and rotary inertia of cross-section. Cheng and Chen (2015) formulated a size-dependent resonance frequency and buckling behavior of nanoplates using the high-order surface stress model. Li *et al*. (2011) employed the strain gradient theory to deal with size effect in transverse bending, vibration and buckling behaviors of nanobeams. Akgöz and Civalek (2015) investigated bending response of functionally graded microbeams embedded in an elastic medium based on modified strain gradient elasticity theory. Mercan and Civalek (2016, 2017) analyzed the buckling behaviour of silicon carbide and boron nitride nanotubes with surface effects. Civalek and Demir (2016) further proposed a simple nonlocal beam model to study buckling response of protein microtubules surrounded by an elastic matrix by nonlocal finite element method. Extending the usual strain gradient and nonlocal beam theories, Shen *et al*. (2012) considered a generalized nonlocal gradient beam and studied the behavior of flexural waves of carbon nanotubes. Based on the Bernoulli-Euler beam theory and high-order surface stress model, the transverse vibration of an axially compressed nanowire embedded in elastic medium is investigated by Zhang *et al*. (2015). Li *et al*. (2016a) used Hamilton's principle to deduce the equations of motion and boundary conditions for free vibration of functionally graded beams within the framework of the nonlocal strain gradient Timoshenko theory. Wu *et al*. (2017) dealt with free and forced vibration of nanowires with the surface effects and demonstrated size-dependent natural frequencies within the framework of the Timoshenko beam theory. Choi *et al*. (2010) employed

*Corresponding author, Ph.D.
E-mail: xfli@csu.edu.cn

ISSN: 1225-4568 (Print), 1598-6217 (Online)

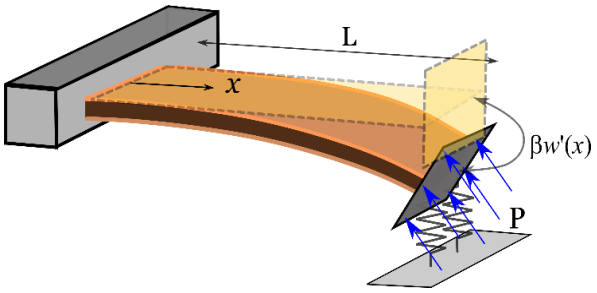

Fig. 1 Schematic of a clamped-elastically restrained nanobeam under a subtangential follower force

finite element method to calculate the natural frequencies and mode shapes of a nanosized thin film with consideration of surface effects. Wang and Wang (2014) analyzed the effect of surface energy on the sensing performance of bridged nanotube-based micro-mass sensors. Ansari *et al*. (2013) coped with the size-dependent vibration of functionally graded curved microbeams on the basis of the modified strain gradient elasticity theory. For a cracked nanobeam, the influence of surface energy on vibration frequency has been studied (Hasheminejad *et al*. 2011, Wang and Wang 2015). Ebrahimi *et al*. (Ebrahimi *et al*. 2016) studied the influence of thermal loading and surface effects on mechanical behavior of nanotubes. For an elastic plate with surface effects, Shaat and Mahmoud (2015) established a new Mindlin functionally graded plate incorporating surface energy. Zhu *et al*. (2014) gave a buckling analysis of an elastic plate with attached thin films with intrinsic stresses. On the other hand, the effect of surface elasticity on the elastic properties of nanowires was confirmed through various approaches (Asthana *et al*. 2011, Yao *et al*. 2012, Zheng *et al*. 2010).

The above-mentioned researches mainly focus on vibration of nanobeams under the condition of conservative forces if any. For the case of nonconservative forces, work on dynamic behavior of nanobeams is very limited, although a large number of studies on classical beam-columns subjected to nonconservative forces have been reported (Elishakoff 2005, Langthjem and Sugiyama 2000). For micro/nano beam-columns, Xiang *et al*. (2010) applied Eringen's nonlocal elasticity theory to investigate the dynamic instability of a nanocantilever under a follower force. Li *et al*. (2016c) studied the influences of surface effects on flutter instability of a nanorod with an additional mass attached to the end. Dynamic stability of microcantilevers with surface effects on an elastic foundation has been addressed when a subtangential follower force is loaded (Li *et al*. 2016b).

This paper aims at the vibration and dynamic stability of a clamped-elastically restrained nanobeam subjected to a nonconservative force or a generalized follower force. Emphasis is placed on the analysis of surface effects on critical divergence and flutter loads. The characteristic equation is firstly derived based on Hamilton's principle. The force-frequency interaction curve is displayed for various directions of applied force and values of spring stiffness. Whether the divergence and flutter instability occur is discussed in detail.

2. Basic equations

A schematic of a clamped-elastically restrained nanobeam with surface effects is shown in Fig. 1. For example, such a structure can be used as a fluid energy harvesting device which consists of a piezoelectric bimorph cantilever. Consider dynamic stability of a nanobeam subjected to a generalized follower force P with tangency coefficient β, which can be used to simulate the situation of some loading such as wind or fluid acting at the surface of a plate at the elastically restraint end. Here, a translational spring is linked to the free end of the nanobeam. Since cantilever beams at nano scale have evident size effects and in the present analysis we invoke the surface elasticity theory to account for the size effects. That is, based on the surface stress-strain relation (Gurtin and Murdoch 1975)

$$\sigma_{\alpha\beta}^{s}=\sigma_0\delta_{\alpha\beta}+(\sigma_0+\lambda^{s})\varepsilon_{\gamma\gamma}\delta_{\alpha\beta}+2(\mu^{s}-\sigma_0)\varepsilon_{\alpha\beta}+\sigma_0 u_{\alpha,\beta}^{s} \quad (1)$$

Where λ^s and μ^s are the Lame constants for surface material and σ_0 is the residual surface stress, we can obtain one-dimensional version as follows

$$\sigma^{s}=\sigma_0+E^{s}\varepsilon^{s}. \quad (2)$$

Recalling the one-dimensional version of the constitutive equation for bulk material

$$\sigma=E\varepsilon, \quad (3)$$

where $\sigma(\varepsilon)$ and $\sigma^s(\varepsilon^s)$ are axial stress (strain) and surface axial stress (strain), respectively, E and E^s represent moduli of bulk and surface elasticity respectively.

Under infinitesimal deformation assumption, the strain energy of a deformed nanobeam can be expressed as

$$\begin{aligned}U&=\frac{1}{2}\int_0^L\left(\int_A\sigma\varepsilon dA+\int_C\sigma^{s}\varepsilon^{s}ds\right)dx+\frac{1}{2}Kw_L^2\\&=\frac{D}{2}\int_0^L\left(\frac{\partial^2 w}{\partial x^2}\right)^2dx+\frac{1}{2}Kw_L^2,\end{aligned} \quad (4)$$

and the kinetic energy is expressed as

$$\begin{aligned}K&=\frac{1}{2}\int_0^L\left[\int_A\rho\left(\frac{\partial w}{\partial t}\right)^2dA+\int_C\rho^{s}\left(\frac{\partial w}{\partial t}\right)^2ds\right]dx\\&=\frac{m}{2}\int_0^L\left(\frac{\partial w}{\partial t}\right)^2dx,\end{aligned} \quad (5)$$

where D denotes effective bending stiffness, m stands for effective mass per unit length, w_L the value of deflection w at $x=L$, K spring stiffness of the elastic restraint end, and

$$D=EI\left(1+\lambda_d\right),\lambda_d=\frac{E^{s}J}{EI}, \quad (6)$$

$$m=\rho A\left(1+\lambda_m\right),\lambda_m=\frac{\rho^{s}C}{\rho A}, \quad (7)$$

$$I=\int_A z^2dA,J=\int_C z^2ds. \quad (8)$$

In the above, L is the beam length, I moment of inertia

of cross section, J moment of inertia of surface cross section (boundary), A cross-sectional area, C the boundary of the cross-section A, ρ mass density, and ρ^s surface mass per unit length. Also, the Euler-Bernoulli beam theory incorporating the surface elasticity is adopted, and the axial strain can be expressed in terms of the deflection w as

$$\varepsilon = -z\frac{\partial^2 w}{\partial x^2}, \tag{9}$$

where the x-axis is longitudinal coordinate along the undeformed axis of the nanobeam, and the positive z axis is normal to the x -axis. The strain energy (4) is composed of two terms, the last term of which arises from the contribution of the elastic restraint end.

A nonconservative load P can be decomposed into a horizontal force component and a vertical force component. The horizontal component $P\cos(\beta w_L^{'})$ approximately equals to P according to the assumption of small deflection. Then the work done by the horizontal component is

$$V = -\frac{1}{2}(P-H)\int_0^L \left(\frac{\partial w}{\partial x}\right)^2 dx, \tag{10}$$

where small axial deformation has been neglected before buckling, and H represents a resultant force of the surface residual tension over cross-section, i.e.

$$H = \int_C \sigma_0 ds. \tag{11}$$

Similarly, the vertical component of the load $P\sin(\beta w_L^{'})$ approximately equals to $P\beta w_L^{'}$, which is nonconservative, and the work done by the vertical component is

$$\delta V_E = -\beta P w_L^{'}\delta w_L, \tag{12}$$

where $w_L^{'}$ denotes the value of dw/dx at $x=L$.

Then, we substitute Eqs. (4), (5), (10) and (12) into Hamilton's principle

$$\delta\int_{t_1}^{t_2}(K-U-V)dt + \int_{t_1}^{t_2}\delta V_E dt = 0, \tag{13}$$

By variational operation, we simultaneously get the governing partial differential equation

$$D\frac{\partial^4 w}{\partial x^4} + (P-H)\frac{\partial^2 w}{\partial x^2} + m\frac{\partial^2 w}{\partial t^2} = 0, \tag{14}$$

and associated boundary conditions

$$w = 0, \frac{\partial w}{\partial x} = 0, x = 0; \tag{15}$$

$$\frac{\partial^2 w}{\partial x^2} = 0, D\frac{\partial^3 w}{\partial x^3} + \left[P(1-\beta) - H\right]\frac{\partial w}{\partial x} - Kw = 0, x = L. \tag{16}$$

We note that if setting spring stiffness K to vanish, the boundary conditions in (16) reduce to the boundary conditions of the free end. Moreover, β=0 corresponds to a conservative force, whereas β=1 gives a case of a tangential follower force (Beck's column).

3. Characteristic equation

In this section, the flutter instability of a clamped-elastically restrained nanobeam subjected to a nonconservative force is studied. For flutter problems, we take the deflectio w having the form $w=W(\xi)Le^{i\omega t}$, where $i=\sqrt{-1}$, $\xi = x/L$, ω is the circular frequency, and W is the dimensionless amplitude. Introduce dimensionless parameters as follows

$$p = \frac{PL^2}{EI},\ \eta = \frac{HL^2}{EI}, \Omega^2 = \frac{\rho A L^4 \omega^2}{EI},\ k = \frac{KL^3}{EI}. \tag{17}$$

Inserting the expression for w into (14) one obtains

$$W^{IV} + \frac{p-\eta}{1+\lambda_d}W'' - \frac{1+\lambda_m}{1+\lambda_d}\Omega^2 W = 0, \tag{18}$$

where the prime represents differentiation with respect to ξ. The boundary conditions given by (15) and (16) become

$$W(0) = 0, W'(0) = 0, \tag{19}$$

$$W''(1) = 0, W'''(1) + \frac{p(1-\beta)-\eta}{1+\lambda_d}W'(1) - \frac{k}{1+\lambda_d}W(1) = 0, \tag{20}$$

Substituting $W(\xi) = e^{\gamma\xi}$ into Eq. (18), we can obtain the following algebraic equation in γ

$$\gamma^4 + \frac{p-\eta}{1+\lambda_d}\gamma^2 - \frac{1+\lambda_m}{1+\lambda_d}\Omega^2 = 0. \tag{21}$$

By solving the above algebraic equation, one obtains two pairs of distinct roots as $\pm\gamma_1$ and $\pm i\gamma_2$, where

$$\gamma_1 = \sqrt{\frac{\sqrt{(p-\eta)^2 + 4(1+\lambda_d)(1+\lambda_m)\Omega^2} - (p-\eta)}{2(1+\lambda_d)}}, \tag{22}$$

$$\gamma_2 = \sqrt{\frac{\sqrt{(p-\eta)^2 + 4(1+\lambda_d)(1+\lambda_m)\Omega^2} + (p-\eta)}{2(1+\lambda_d)}}. \tag{23}$$

With the above roots, it is a simple matter to write a general solution of Eq. (18) as

$$W = C_1\cosh(\gamma_1\xi) + C_2\sinh(\gamma_1\xi) + C_3\cos(\gamma_2\xi) + C_4\sin(\gamma_2\xi), \tag{24}$$

where C_1, C_2, C_3 and C_4 are four unknown constants to be determined through boundary conditions. To this end, substitution of (24) into the boundary conditions (19) and (20) gives

$$C_1 + C_3 = 0, \tag{25}$$

$$C_2\gamma_1 + C_4\gamma_2 = 0, \tag{26}$$

$$\gamma_1^2(C_1\cosh\gamma_1 + C_2\sinh\gamma_1) - \gamma_2^2(C_3\cos\gamma_2 + C_4\sin\gamma_2) = 0, \tag{27}$$

$$B_1C_1 + B_2C_2 + B_3C_3 - B_4C_4 = 0, \tag{28}$$

where

$$B_1 = \gamma_1\left(\gamma_2^2 - \frac{p\beta}{1+\lambda_d}\right)\sinh\gamma_1 - \frac{k}{1+\lambda_d}\cosh\gamma_1 \tag{29}$$

$$B_2=\gamma_1\left(\gamma_2^2-\frac{p\beta}{1+\lambda_d}\right)\cosh\gamma_1-\frac{k}{1+\lambda_d}\sinh\gamma_1 \tag{30}$$

$$B_3=\gamma_2\left(\gamma_1^2+\frac{p\beta}{1+\lambda_d}\right)\sin\gamma_2-\frac{k}{1+\lambda_d}\cos\gamma_2 \tag{31}$$

$$B_4=\gamma_2\left(\gamma_1^2+\frac{p\beta}{1+\lambda_d}\right)\cos\gamma_2+\frac{k}{1+\lambda_d}\sin\gamma_2. \tag{32}$$

The determinant of the coefficient matrix has to vanish because of the existence of a non-trivial solution of the system of algebraic equations. We can obtain, after some algebraic manipulations, the characteristic equation can be obtained as follows

$$\begin{aligned}&1+A_1\cosh\gamma_1\sin\gamma_2+A_2\cosh\gamma_1\cos\gamma_2\\&-A_3\sinh\gamma_1\sin\gamma_2-A_4\sinh\gamma_1\cos\gamma_2=0\end{aligned} \tag{33}$$

where

$$A_1=\frac{k\gamma_1(1+\lambda_d)^{\frac{5}{2}}\sqrt{(p-\eta)^2+4(1+\lambda_d)(1+\lambda_m)\Omega^2}}{[p\beta(p-\eta)+2(1+\lambda_d)(1+\lambda_m)\Omega^2]\sqrt{1+\lambda_m}\Omega} \tag{34}$$

$$A_2=\frac{\left[p\left(1-\beta\right)-\eta\right](p-\eta)+2(1+\lambda_d)(1+\lambda_m)\Omega^2}{p\beta(p-\eta)+2(1+\lambda_d)(1+\lambda_m)\Omega^2} \tag{35}$$

$$A_3=\frac{(p-\eta-2p\beta)\sqrt{(1+\lambda_d)(1+\lambda_m)}\Omega}{p\beta(p-\eta)+2(1+\lambda_d)(1+\lambda_m)\Omega^2} \tag{36}$$

$$A_4=\frac{k\gamma_2(1+\lambda_d)^{\frac{5}{2}}\sqrt{(p-\eta)^2+4(1+\lambda_d)(1+\lambda_m)\Omega^2}}{[p\beta(p-\eta)+2(1+\lambda_d)(1+\lambda_m)\Omega^2]\sqrt{1+\lambda_m}\Omega}. \tag{37}$$

The characteristic Eq. (33) governs dynamic behavior of a clamped-elastically restrained nanobeam subjected to a nonconservative force at the elastically restrained end.

Here consider two limiting cases $k\to0$ and $k\to\infty$. The former corresponds to a clamped-free nanocantilever, whereas the latter corresponds to a clamped-hinged nanobeam. For the former case, the characteristic Eq. (33) simplifies to

$$\begin{aligned}&1+\frac{\left[p\left(1-\beta\right)-\eta\right](p-\eta)+2(1+\lambda_d)(1+\lambda_m)\Omega^2}{p\beta(p-\eta)+2(1+\lambda_d)(1+\lambda_m)\Omega^2}\cosh\gamma_1\cos\gamma_2\\&-\frac{(p-\eta-2p\beta)\sqrt{(1+\lambda_d)(1+\lambda_m)}\Omega}{p\beta(p-\eta)+2(1+\lambda_d)(1+\lambda_m)\Omega^2}\sinh\gamma_1\sin\gamma_2=0,\end{aligned} \tag{38}$$

identical to that derived in (Li *et al*. 2016c) in the absence of attached mass. Furthermore, in the limiting case of the frequency $\Omega\to0$, Eq. (38) becomes

$$p\beta+\left[p\left(1-\beta\right)-\eta\right]\cos\sqrt{\frac{p-\eta}{1+\lambda_d}}=0, \tag{39}$$

which may be used to determine the divergence loads of a clamped-free nanocantilever under a nonconservative force.

For the latter case, i.e., $k\to\infty$, the system is a clamped-hinged column. Evidently, there is no transverse displacement at the hinged end, even subject to a subtangential follower force. It is readily found that if setting $k\to\infty$, the characteristic Eq. (33) reduces to

$$\gamma_1\tan\gamma_2-\gamma_2\tanh\gamma_1=0 \tag{40}$$

This equation governs the dynamic behavior of a clamped-hinged nanobeam.

In addition, as a check, we let surface effects disappear, that is to say E^s=0, ρ^s=0 and σ_0=0. Under such circumstances, we find

$$\begin{aligned}&\lambda_d=\lambda_m=0,\eta=0,\\&\gamma_1=\sqrt{\frac{\sqrt{p^2+4\Omega^2}-p}{2}},\gamma_2=\sqrt{\frac{\sqrt{p^2+4\Omega^2}+p}{2}},\end{aligned} \tag{41}$$

and the characteristic Eq. (33) simplifies to

$$\begin{aligned}&1+\frac{2\Omega^2+p^2\left(1-\beta\right)}{2\Omega^2+p^2\beta}\cosh\gamma_1\cos\gamma_2-\frac{p\Omega\left(1-2\beta\right)}{2\Omega^2+p^2\beta}\sinh\gamma_1\sin\gamma_2\\&-\frac{k\sqrt{p^2+4\Omega^2}}{(2\Omega^2+p^2\beta)\Omega}\gamma_2\sinh\gamma_1\cos\gamma_2+\frac{k\sqrt{p^2+4\Omega^2}}{(2\Omega^2+p^2\beta)\Omega}\gamma_1\cosh\gamma_1\sin\gamma_2=0,\end{aligned} \tag{42}$$

which is in exact agreement with that for flutter instability of a classical Euler-Bernoulli beam (Pedersen 1977, Sundararajan 1976). In particular, the characteristic Eq. (38) for k=0 in the absence of surface effects reduces to

$$1+\frac{2\Omega^2+p^2\left(1-\beta\right)}{2\Omega^2+p^2\beta}\cosh\gamma_1\cos\gamma_2-\frac{p\Omega\left(1-2\beta\right)}{2\Omega^2+p^2\beta}\sinh\gamma_1\sin\gamma_2=0, \tag{43}$$

in accordance with that reported in (Chen 2003). In the following analysis, we see how the surface effects affect flutter instability of a clamped-elastically restrained nanobeam under a nonconservative force.

4. Numerical results

In this section, numerical computations are performed to illustrate the effect of surface effects on the flutter instability of a clamped-elastically restrained nanobeam. The values of surface elastic modulus and surface stress are reported in some papers (Ibach 1997, Shenoy 2005). Here, we choose a nanobeam with material properties λ=μ=22.5 GPa, ρ=3×10^3 kg/m^3, σ_0=110 N/m, λ^s=7×10^3 N/m, μ^s=8×10^3 N/m, ρ^s=7×10^{-4} kg/m^2 (Gurtin and Murdoch 1978). From these material constants, we can evaluate Young's modulus and Poisson's ratio for the bulk material and surface material. We can easily obtain, for rectangular cross-section with height h and breadth b

$$C=2\left(b+h\right),A=bh,I=\frac{1}{12}bh^3,J=\frac{bh^2}{2}+\frac{h^3}{6}, \tag{44}$$

and for circular cross-section with diameter d

$$C=\pi d,A=\frac{1}{4}\pi d^2,I=\frac{1}{64}\pi d^4,J=\frac{\pi d^3}{8} \tag{45}$$

The geometric parameters used in the following are length L=180 μm, diameter d=20 μm. From the above we get the values of λ_d, λ_m and η.

First numerical results for a clamped-free nanobeam and a clamped-hinged nanobeam corresponding to $k\to0$ and $k\to\infty$, respectively, are calculated. In fact, they are two limit

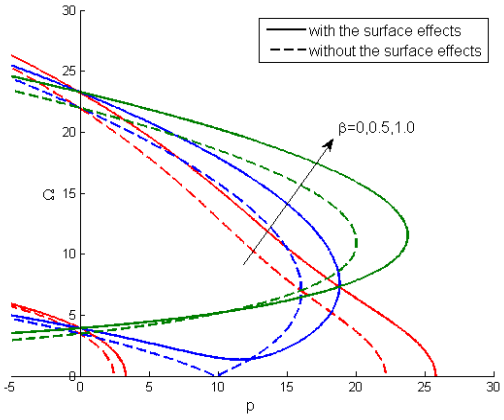

Fig. 2 The force-frequency interaction curves for clamped free nanobeam with and without surface effects

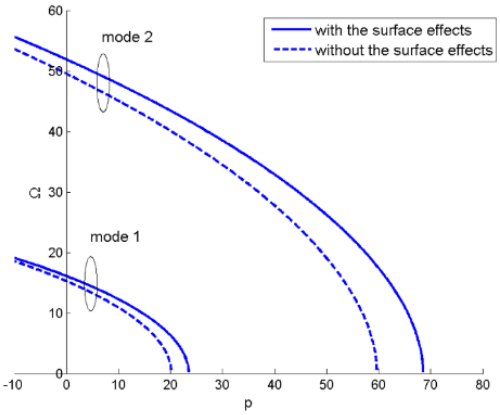

Fig. 3 The force-frequency interaction curves for a clamped-hinged nanobeam with and without surface effects

cases of an elastically restrained nanobeam. Fig. 2 shows the interaction between the dimensionless frequency parameter Ω and the subtangential follower force parameter p for a clamped-free nanobeam. In the following, three typical interaction curves are displayed, i.e., β=0,0.5,1, where β=0 corresponds to the case of a conservative force, and β=1 corresponds to the case of a usual tangential follower force (Beck's column). On the other hand, the force parameter p may be positive or negative, p>0 indicates compressive follower force and p<0 a tensile follower force. From Fig. 2, it is seen that for the case of β=0, there are two distinct curves, corresponding to the first and the second mode of vibration, regardless of the surface effect included (solid lines) or excluded (dashed lines), while for β=0.5 or 1, two curves coalesce to a continuous curve. These two cases represent two different characteristics. For various values of β, i.e., β=0,0.5,1, the first- and second-order natural frequencies can be given from the first and second intersecting locations of the force-frequency interaction curve with the Ω -axis, respectively, i.e., Ω_1=3.516 and Ω_2=22.034, in exact agreement with the well-known results (Pilkey 1994). When taking the surface effects into consideration (solid lines), the values of the first two frequencies Ω_1 and Ω_2 are added to 3.962 and 23.333, respectively.

Table 1 Dimensionless critical loads of a clamped-free nanobeam under a subtangential follower force

β		with the surface effects	without the surface effects	(Mutyalarao *et al*. 2013)
Divergence	0	3.3272	2.4709	2.4675
	0.1	3.8116	2.8300	2.8297
	0.2	4.4825	3.3255	3.3252
	0.3	5.4799	4.0554	4.0552
	0.4	7.2277	5.2926	5.2930
Flutter	0.5	18.8147	16.0523	16.0547
	0.6	19.1219	16.2589	16.2607
	0.7	19.7935	16.7874	16.7891
	0.8	20.7819	17.5887	17.5903
	0.9	22.0963	18.6680	18.6689
	1.0	23.7612	20.0506	20.0522
	1.2	28.1925	23.7971	-
	1.5	35.9358	30.6282	-

Similarly, for β=0, the first and second divergence loads can be determined from the first and second intersecting locations of the force-frequency interaction curve with the p-axis. Nevertheless, for β values larger than 0.5, the intersecting locations of the force-frequency interaction curve with the p-axis disappear and in this case divergence load does not exist. Divergence instability at zero frequency does not occur. Instead, flutter instability happens at a nonvanishing frequency. That is, for a larger value of β, e.g., β>0.5, two curves coalesce to a continuous curve, and there is a maximum positive value of p at the force-frequency interaction curve, which just corresponds to the flutter load. For example, the maximum p values of the force-frequency interaction curve for β=0.5,1 are about p_{cr}=16.052, 20.051, respectively, for dashed lines. For solid lines, a similar feature is also observed. Moreover, more interesting is that all the dashed or solid curves have an intersecting common point at about p_{cr}=16 or 18.8. This is to say that there exists a minimum flutter critical load for possible tangency coefficients, coinciding with that observed in (Li *et al*. 2016c). In addition, compressive force may give rise to occurrence of flutter instability, and tensile force obviously does not cause flutter instability. However, for combined forces consisting of tensile and compressive forces, occurrence of flutter instability still possible (Leung, 2008). For those p values less than the flutter load, harmonic vibration takes place. In particular it is viewed that tensile subtangential forces (p<0) gives an increase in the natural frequencies of a nanocantilever for small values of β, which is understood in the way that a nanocantilever under a tensile force looks like stiffer and gives higher natural frequencies. However, for β=1, a tensile tangential follower force decreases the first frequency and increases the second frequency, as seen in Fig. 2. When the surface effects are taken into account, the natural frequencies, divergence and flutter loads increase. Here, Table 1 lists critical loads for a clamped-free nanobeam with and without surface effects for typical tangency coefficients. We can see that the results in the absence of surface effects agree well with those given in (Mutyalarao *et al*. 2013).

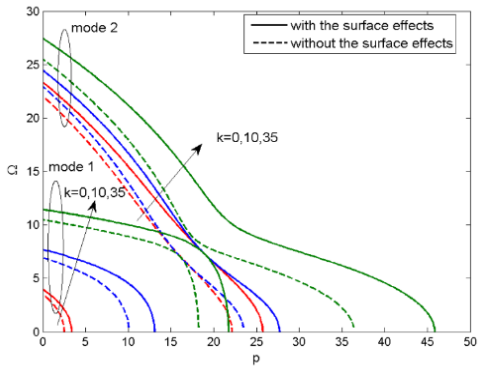

(a)

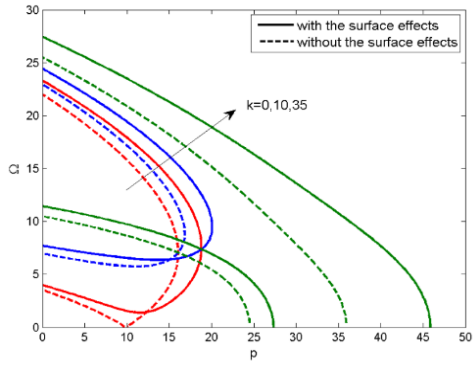

(b)

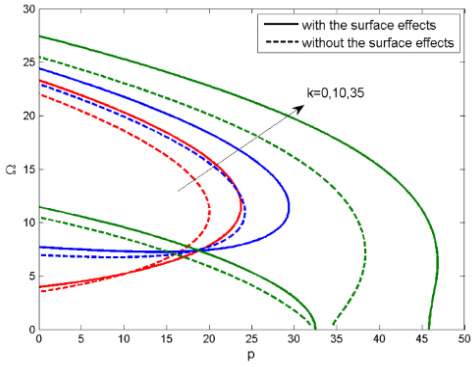

(c)

Fig. 4 The force-frequency relationship curves for a clamped-elastically restrained nanobeam with and without surface effects, (a) β=0, (b) β=0.5, (c) β=1

For another limit case of $k\to\infty$, Fig. 3 shows the force-frequency interaction curves of a clamped-hinged nanobeam with and without the surface effects. From the expression in (40), we notice that the system is independent of β. As viewed in Fig. 3, the system has the divergence instability type alone with divergence loads at the p-axis intersecting locations of these curves.

Next, let us discuss dynamic stability of a general nanocantilever linked to a translational spring. In Figs. 4(a)-(c), the force-frequency interaction curves are presented for three different values of spring stiffness k=0,10,35 for a conservative force, a subtangential follower force, and a tangential follower force, respectively. For the case of β=0, divergence instability occurs but flutter instability does not, as seen in Fig. 4(a). The divergence loads and natural

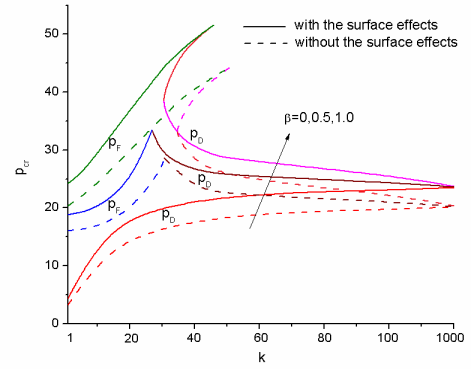

Fig. 5 Critical loads versus spring stiffness parameter for three different tangency coefficients β=0,0.5,1

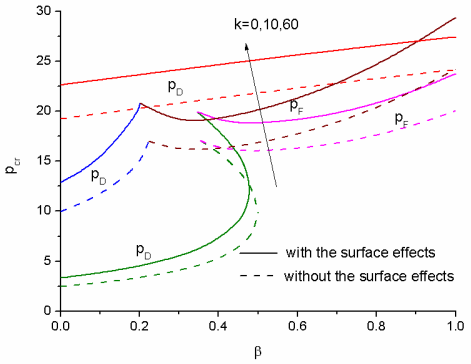

Fig. 6 Critical loads versus the tangency coefficient β for different spring stiffness parameters, k=0,10,60

frequencies increase with the increasing of spring stiffness, and the surface effects have an enhancing trend. From Fig. 4(b) and (c), for β=0.5,1.0, whether flutter instability takes place depends on the tangency coefficient and spring stiffness. Or rather, for smaller spring stiffness (e.g., k<10) rather than larger ones (e.g., k=35), flutter instability readily occurs for a clamped-elastically restrained nanobeam. When the spring stiffness is gradually raised to be relatively large (e.g., k=35), the flutter instability transits to divergence instability at a certain spring stiffness. It is interesting to mention that there is still a dimensionless frequency parameter Ω corresponding to the intersection point of the curves, regardless of the presence and absence of the surface effects, and moreover, this frequency parameter is Ω_{cr}=7.36 for the surface effects are taken into account and Ω_{cr}=7.06 for the surface effects are excluded, which is independent of β and k. This phenomenon coincides with that pointed out in (Pedersen 1977). As mentioned before, the corresponding p_{cr} value at the intersection point actually gives the minimum flutter load if flutter instability occurs (Li *et al*. 2016c).

For clarity, the influence of the spring stiffness parameter k on the critical load of a clamped-elastically restrained nanobeam with three tangency coefficients β=0.5,1.0 is illustrated in Fig. 5. Here the critical load refers to the divergence load denoted as p_D and the flutter load denoted as p_F in Fig. 5. Since there is only divergence instability for any k value in the case of β=0, in Fig. 5 the critical divergence load monotonically increases with the

increasing of spring stiffness. However, by observing the critical load curves for β=0.5,1, we find that it is completely different from the above trend and critical flutter load for β=0.5 gradually rises up to a value of about k=30.62 with the spring stiffness rising. At this position, there is a sudden drop in the critical load as k is further raised and the instability type transfers from flutter to divergence. From this point onwards, the increase of k gives rise to the decrease of divergence critical load. The critical load curve for β=1 has a trend similar to that for β=0.5. We note a difference that there exists a range: 34.8<k<51.6, in which flutter and divergence instability appear simultaneously, but divergence instability takes place firstly. For sufficiently large spring stiffness, all critical load curves intersect at a common point, meaning that the critical divergence loads are independent of β and in fact correspond to the Euler buckling loads of a clamped-hinged nanobeam with and without the surface effects. This is in line with that observed in Fig. 3. For solid lines, the critical loads with consideration of the surface effects obviously increase.

Finally, we examine the effect of the tangency coefficient on the critical load. Fig. 6 gives the critical load as a function of β for k=0, 10, 60. In the case of k=0, the critical divergence load p_D increases monotonically with an increase of β and the curve has an inflexion point at about β=0.5. It is worth noting that at this particular value of β≈0.5, the type of instability suddenly changes from divergence to flutter, as pointed out in (Chen 2003). Later with an increase of β, the critical flutter load decreases slightly at first and then increases, that is, there is a minimum value of critical flutter load for a certain value of β. For k=10 a similar phenomenon is observed. For k=60, the instability type exhibits only divergence type and no flutter occurs. Moreover, the critical divergence load increases monotonically as k increases. The critical loads for solid curves (with the surface effects) significantly increase.

5. Conclusions

This paper investigated the influences of surface properties and spring stiffness of the restraint end on the dynamic behavior of a clamped-elastically restrained nanobeam under the action of a subtangential follower force. We first employed Hamilton's principle and derived the characteristic equation governing the force-frequency interaction. Based on the resulting equation, the influences of the surface effects, spring stiffness on the critical loads were analyzed. Some conclusions are drawn as follows:

- The surface properties evidently change critical loads and natural frequencies, as well as the type of instability of a nanocantilever.
- For a clamped-hinged nanobeam, only divergence instability exists and divergence loads are independent of β.

For a conservative force, divergence instability of system always occurs, regardless of the value of spring stiffness.

- For a nonconservative force, the spring stiffness plays a dominated role of instability type. Flutter instability and divergence instability can transit when the tangency coefficient of applied force and the spring stiffness are changed.

Acknowledgements

This work was supported by the National Natural Science Foundation of China (No. 11672336) and the Open Foundation of State Key Laboratory of Structural Analysis for Industrial Equipment, Dalian University of Technology, PRC (No. GZ1712)

References

Akgoz, B. and Civalek, O. (2015), ‘‘Bending analysis of FG microbeams resting on Winkler elastic foundation via strain gradient elasticity”, *Compos. Struct.*, **134**, 294-301.

Ansari, R., Gholami, R. and Sahmani, S. (2013), ‘‘Size-dependent vibration of functionally graded curved microbeams based on the modified strain gradient elasticity theory”, *Arch. Appl. Mech.*, **83**(10), 1439-1449.

Asthana, A., Momeni, K., Prasad, A., Yap, Y.K. and Yassar, R.S. (2011), “In situ observation of size-scale effects on the mechanical properties of ZnO nanowires”, *Nanotechnol.*, **22**(26), 265712.

Chen, Y.Z. (2003), “Interaction between compressive force and vibration frequency for a varying cross-section cantilever under action of generalized follower force”, *J. Sound Vib.*, **259**(4), 991-999.

Cheng, C.H. and Chen, T. (2015), “Size-dependent resonance and buckling behavior of nanoplates with high-order surface stress effects”, *Physica E*, **67**, 12-17.

Choi, J., Cho, M. and Kim, W. (2010), “Surface effects on the dynamic behavior of nanosized thin film resonator”, *Appl. Phys. Lett.*, **97**(97), 171901.

Civalek, O. and Demir, C. (2016), “A simple mathematical model of microtubules surrounded by an elastic matrix by nonlocal finite element method”, *Appl. Math. Comput.*, **289**, 335-352.

Cuenot, S., Fretigny, C., Demoustier-Champagne, S. and Nysten, B. (2004), “Surface tension effect on the mechanical properties of nanomaterials measured by atomic force microscopy”, *Phys. Rev. B*, **69**(16), 165410.

Ebrahimi, F., Shaghaghi, G.R. and Boreiry, M. (2016), “An investigation into the influence of thermal loading and surface effects on mechanical characteristics of nanotubes”, *Struct. Eng. Mech.*, **57**(1), 179-200.

Elishakoff, I. (2005), “Controversy associated with the so-called “follower forces”: Critical overview”, *Appl. Mech. Rev.*, **58**(2), 117-142.

Gurtin, M.E. and Murdoch, A.I. (1975), “A continuum theory of elastic material surfaces”, *Arch. Ration. Mech. Anal.*, **57**(4), 291-323.

Gurtin, M.E. and Murdoch, A.I. (1978), “Surface stress in solids”, *Int. J. Solid. Struct.*, **14**(6), 431-440.

Hasheminejad, B.S.M., Gheshlaghi, B., Mirzaei, Y. and Abbasion, S. (2011), “Free transverse vibrations of cracked nanobeams with surface effects”, *Thin Solid Film.*, **519**(8), 2477-2482.

Ibach, H. (1997), “The role of surface stress in reconstruction, epitaxial growth and stabilization of mesoscopic structures”, *Surf. Sci. Rep.*, **29**(5-6), 195 - 263.

Jing, G.Y., Duan, H.L., Sun, X.M., Zhang, Z.S., Xu, J., Li, Y.D., Wang, J.X. and Yu, D.P. (2006), “Surface effects on elastic

properties of silver nanowires: Contact atomic-force microscopy", *Phys. Rev. B*, **73**(23), 235409.
Lachut, M.J. and Sader, J.E. (2007), "Effect of surface stress on the stiffness of cantilever plates", *Phys. Rev. Lett.*, **99**(20), 206102.
Langthjem, M.A. and Sugiyama, Y. (2000), "Dynamic stability of columns subjected to follower loads: A survey", *J. Sound Vib.*, **238**(5), 809-851.
Leung, A.Y.T. (2008), "Exact spectral elements for follower tension buckling by power series", *J. Sound Vib.*, **309**(3-5), 718-729.
Li, L., Li, X. and Hu, Y. (2016a), "Free vibration analysis of nonlocal strain gradient beams made of functionally graded material", *Int. J. Eng. Sci.*, **102**, 77-92.
Li, X.F., Jiang, S.N. and Lee, K.Y. (2016b), "Surface effect on dynamic stability of microcantilevers on an elastic foundation under a subtangential follower force", *Int. J. Mech. Mater. Des.*, doi:10.1007/s10999-016-9362-1.
Li, X.F., Wang, B.L., Tang, G.J. and Lee, K.Y. (2011), "Size effect in transverse mechanical behavior of one-dimensional nanostructures", *Physica E*, **44**(1), 207-214.
Li, X.F., Zhang, H. and Lee, K.Y. (2014), "Dependence of Young's modulus of nanowires on surface effect", *Int. J. Mech. Sci.*, **81**, 120-125.
Li, X.F., Zou, J., Jiang, S.N. and Lee, K.Y. (2016c), "Resonant frequency and flutter instability of a nanocantilever with the surface effects", *Compos. Struct.*, **153**, 645-653.
Mercan, K. and Civalek, O. (2016), "Dsc method for buckling analysis of boron nitride nanotube (BNNT) surrounded by an elastic matrix", *Compos. Struct.*, **143**, 300-309.
Mercan, K. and Civalek, O. (2017), "Buckling analysis of Silicon carbide nanotubes (SiCNTs) with surface effect and nonlocal elasticity using the method of HDQ", *Compos. Part B*, **114**, 34-45.
Moon, W. and Hwang, H. (2008), "Atomistic study of structures and elastic properties of single crystalline ZnO nanotubes", *Nanotechnol.*, **19**(22), 225703.
Mutyalarao, M., Bharathi, D. and Rao, B.N. (2013), "Dynamic stability of cantilever columns under a tip-concentrated subtangential follower force", *Math. Mech. Solid.*, **18**(5), 449-463.
Park, H.S. (2008), "Surface stress effects on the resonant properties of silicon nanowires", *J. Appl. Phys.*, **103**(12), 123504.
Pedersen, P. (1977), "Influence of boundary conditions on the stability of a column under non-conservative load", *Int. J. Solid. Struct.*, **13**(5), 445-455.
Pilkey, W.D. (1994), *Formulas for Stress, Strain, and Structural Matrices*, John Wiley & Sons, Inc.
Shaat, M. and Mahmoud, F.F. (2015), "A new Mindlin FG plate model incorporating microstructure and surface energy effects", *Struct. Eng. Mech.*, **53**(1), 105-130.
Shen, J., Wu, J.X., Song, J., Li, X.F. and Lee, K.Y. (2012), "Flexural waves of carbon nanotubes based on generalized gradient elasticity", *Phys. Stat. Sol. B*, **249**(1), 50-57.
Shenoy, V.B. (2005), "Atomistic calculations of elastic properties of metallic fcc crystal surfaces", *Phys. Rev. B*, **71**(9), 094104.
Shi, M.X., Liu, B., Zhang, Z.Q., Zhang, Y.W. and Gao, H.J. (2012), "Direct influence of residual stress on the bending stiffness of cantilever beams", *Proc. R. Soc. A*, **468**(2145), 2595-2613.
Sundararajan, C. (1976), "Influence of an elastic end support on the vibration and stability of Beck's column", *Int. J. Mech. Sci.*, **18**(5), 239-241.
Wang, G.F. and Feng, X.Q. (2007), "Effects of surface elasticity and residual surface tension on the natural frequency of microbeams", *Appl. Phys. Lett.*, **90**(23), 231904.
Wang, J., Huang, Z., Duan, H., Yu, S., Feng, X., Wang, G., Zhang, W. and Wang, T. (2011), "Surface stress effect in mechanics of nanostructured materials", *Acta Mech. Solida Sin.*, **24**(1), 52-82.
Wang, K. and Wang, B. (2015), "Timoshenko beam model for the vibration analysis of a cracked nanobeam with surface energy", *J. Vib. Control*, **21**(12), 2452-2464.
Wang, K.F. and Wang, B. (2014), "Effect of surface energy on the sensing performance of bridged nanotube-based micro-mass sensors", *J. Intell. Mater. Syst. Struct.*, **25**(17), 2177-2186.
Wu, J.X., Li, X.F., Tang, A.Y. and Lee, K.Y. (2017), "Free and forced transverse vibration of nanowires with surface effects", *J. Vib. Control*, **23**(13), 2064-2077.
Xiang, Y., Wang, C.M., Kitipornchai, S. and Wang, Q. (2010), "Dynamic instability of nanorods/nanotubes subjected to an end follower force", *J. Eng. Mech.*, **136**(8), 1054-1058.
Yao, H., Yun, G., Bai, N. and Li, J. (2012), "Surface elasticity effect on the size-dependent elastic property of nanowires", *J. Appl. Phys.*, **111**(8), 083506.
Zang, X., Zhou, Q., Chang, J., Liu, Y. and Lin, L. (2015), "Graphene and carbon nanotube (CNT) in MEMS/NEMS applications", *Microelectron. Eng.*, **132**, 192-206.
Zhang, Y.Q., Pang, M. and Chen, W.Q. (2015), "Transverse vibrations of embedded nanowires under axial compression with high-order surface stress effects", *Physica E*, **66**, 238-244.
Zheng, X.P., Cao, Y.P., Li, B., Feng, X.Q. and Wang, G.F. (2010), "Surface effects in various bending-based test methods for measuring the elastic property of nanowires", *Nanotechnol.*, **21**(20), 205702.
Zhu, J., Yang, J.S. and Ru, C.Q. (2014), "Buckling of an elastic plate due to surface-attached thin films with intrinsic stresses", *Struct. Eng. Mech.*, **52**(1), 89-95.

PL